Submitted to

31st International Conference on High Energy Physics, ICHEP02, July 24, 2002, Amsterdam

Abstract: **997**

Parallel Session **6**

www-h1.desy.de/h1/www/publications/conf/conf_list.html

Investigation of Pomeron- and Odderon Induced Photoproduction of Mesons Decaying to Pure Multiphoton Final States at HERA

H1 Collaboration

Abstract

This paper reports on cross section measurements made at HERA for the reactions $\gamma p \to \omega p$ and $\gamma p \to \omega \pi^0 X$, and on searches for the reactions $\gamma p \to \pi^0 N^*$, $\gamma p \to f_2(1270)X$, and $\gamma p \to a_2^0(1320)X$, where N^* denotes an excited nucleon state. The average photon - proton centre-of-mass energy at HERA were $\langle W \rangle = 200$ GeV and 210 GeV. Cross sections for the Pomeron - mediated reactions were determined in agreement with previous measurements and theoretical expectations. Processes mediated by Odderon - photon fusion could not be observed; upper limits on cross sections are below predictions from a non-perturbative QCD model.

1 Introduction

The Pomeranchuk trajectory ("Pomeron", $I\!P$) was introduced, in the framework of Regge theory, in order to explain the high energy behaviour of hadron-hadron scattering. It was named after I. Ya. Pomeranchuk whose famous conjecture ("Pomeranchuk Theorem" [1]) states that, in the limit of very large energies, the difference between particle-particle and particle-antiparticle total cross sections vanishes.

The Pomeranchuk theorem might, however, be violated by means of an additional "odd under crossing" trajectory which contributes with different signs to particle-particle and particle-antiparticle total cross sections, and thus leads to a finite difference in these cross sections at high energies [2]. No effects of this trajectory named "Odderon" ($I\!\!O$) have been experimentally observed so far. The Pomeron and the Odderon are believed to be close relatives inasmuch as both trajectories are given the same intercept (close to one) and the same slope. In short, the soft (non-perturbative) Odderon is introduced in elastic hadron-hadron scattering as the $C = P = -1$ partner of the Pomeron. Fig. 1 shows a generic graph which describes photon - Pomeron and photon - Odderon induced exclusive processes.

The HERA electron beam acts as an intense source of quasi-real photons. The interactions of these with the proton beam provide a unique opportunity to study the photoproduction of mesons at very high energy. Vector meson production, mediated by Pomeron exchange, has been extensively investigated. Pseudoscalar or tensor mesons cannot be produced via Pomeron exchange, but require the Odderon with its ($C = -1$) - assignment. Thus, HERA offers the possibility to simultaneously investigate Pomeron- and Odderon induced processes, both of which we will call "diffractive" because of the similarity of the trajectories, and the lack of colour- or isospin exchange in these reactions.

This paper reports on cross section measurements for the reactions $\gamma p \to \omega p$ and $\gamma p \to \omega\pi^0 X$, and on searches for the reactions $\gamma p \to \pi^0 N^*$, $\gamma p \to f_2(1270)X$, and $\gamma p \to a_2^0(1320)X$. N^* denotes an ($I = 1/2$) - nucleonic state. The former two processes are mediated by Pomeron exchange and have been observed before [4], the latter three are believed to proceed via photon - Odderon fusion and have not been observed so far.

A common feature of all the above reactions is that the mesons produced are reconsructed from their decays to pure photon final states with the help of the H1 backward calorimeters: The neutral pion decays into two photons with a branching ratio (BR) of 98.8 %, the ω meson decays into $\pi^0\gamma$ with a BR of 8.5 %, the $f_2(1270)$ decays into π π with a BR of 84.7 %, and hence into $\pi^0\pi^0$ with a BR of 84.7 %/3 = 28.2 %. the $a_2^0(1320)$ decays into $\pi^0\eta$ with a BR of 14.5 %, and the η meson decays into two photons with a BR of 39.3 % [5]. A possible source for an exclusive $\omega\pi^0$ final state is the $b_1(1235)$ which decays dominantly into these particles. Considering only meson decays to net multiphoton final states, one classifies these simply according to their C - parity eigenvalues: Vector- and axial vector - mesons, with an odd number of final state photons, carry odd C - parity, while pseudoscalar and tensor mesons, with an even number of final state photons, carry even C - parity. The C - parity of the meson determines its production mechanism via either Pomeron (even C - parity) or Odderon (odd C - parity) exchange between the proton and the final state meson.

Total cross sections have been measured with good precision up to high energies, and their behaviour as a function of energy can be described well by phenomenological models such as that of Donnachie and Landshoff [6] or Cudell [7]. These were extended to describe elastic vector meson production by Schuler and Sjöstrand [8] and were used here to parametrize the cross section for $\gamma p \rightarrow \omega\, p$.

For Odderon induced processes, there exist some predictions which have to be confronted with experiment [9, 10]. The non - observation of Odderon contributions in proton - proton and proton - antiproton reactions is, in these models, explained using a possible quark - diquark structure of the proton which leads to a suppression of the proton - Odderon coupling due to parity arguments.

For quantitative predictions a model in the framework of non-perturbative QCD, the Stochastic Vacuum Model (SVM) [11], is used and applied to high energy scattering by functional methods [12] in which the proton is treated as a quark-diquark system in transverse space. At HERA, a sizeable Odderon contribution to single pseudoscalar or tensor meson photoproduction is expected if simultaneously the proton is excited into an $(I = 1/2)$ – nucleonic state with negative parity.

SVM Model calculations were performed at a photon - proton centre-of-mass energy $W = 20$ GeV [9, 10, 11, 12]. For the extrapolation to HERA energies, the intercept of the Odderon trajectory was assumed as $\alpha(t = 0) = 1$ which leads to an energy independent cross section.

2 Event Selection

All mesons investigated in these analyses have decay channels to pure photonic final states, either through intermediate π^0 or η mesons or directly: The number of final state photons varies between two and five. Since in diffractive photoproduction the quasi-elastically produced mesons take over the incoming photon's energy and momentum, the decay products are detected in the "backward" region of the detector, i.e. in the electron beam direction. At H1 (for a general description see [13]), part of this region is covered by two electromagnetic calorimeters, the SpaCal [14] ("Spaghetti Calorimeter" at $z \approx -155$ cm) and the VLQ [15] ("Very Low Q^2 calorimeter" at $z \approx -302$ cm). Here z represents the distance from the nominal interaction point.

The analyses presented here are based on data taken in 1996 where electrons of 27.56 GeV were collided with protons of 820 GeV, and on data taken in 1999 and 2000 where electrons (respectively positrons) were collided with a proton beam of 920 GeV. The data correspond to integrated luminosities of 4.5 pb^{-1} and 30.6 pb^{-1}, respectively. Photoproduction events with $Q^2 < 0.01$ GeV^2 and $0.3 < y < 0.7$ ($Q^2 = 4EE' \cos^2\theta/2$, $y = 1 - E'/E$, where E and E' are the energies of the incoming and scattered electron, respectively, and θ is the scattering angle measured w.r.t. the proton beam direction) were selected by measuring the almost undeflected electron in a low-angle electron detector 33 m downstream from the interaction point.

The analysis of the reaction $\gamma p \to \pi^0\ N^*$ differs from the others by its trigger conditions: In that, in addition to the general photoproduction condition, an energy deposit of at least 6 GeV in the VLQ and a hit in the Forward Neutron Calorimeter (FNC) with an energy deposition of more than 100 GeV were required. The last requirement ensures the presence of an intermediate excited nucleonic state N^*. (Only N^*'s are believed to lead to a considerable contribution since Regge exchange decreases strongly at high energies, and the production of Δ baryons and the transformation of a proton into a neutron - without excitation - require isospin and charge exchange, respectively.) Neutral pions in this reaction are reconstructed from two photons where a) either both are found in the VLQ, or b) one photon is found in the SpaCal, and the second in the VLQ. A photon in the SpaCal or the VLQ is experimentally defined as a cluster with an energy larger than 90 MeV (100 MeV for the 1996 data) or 2 GeV, respectively. To ensure exclusive production of the final state mesons, no further cluster in the above calorimeters or any charged particle in the track detectors, from which an interaction vertex can be reconstructed, is allowed. As there are no charged particles in the events the position of the vertex cannot be measured, and the kinematics is reconstructed using the nominal interaction vertex. A more detailed description of the investigation of the reaction $\gamma p \to \pi^0\ N^*$ can be found in [16]. The π^0 data sample has been collected during the 1999 - 2000 run period with a proton beam energy of 920 GeV. This corresponds to an average γp centre-of-mass energy $\langle W \rangle = 210$ GeV. All other analyses were carried out at a lower proton beam energy leading to $\langle W \rangle = 200$ GeV.

In the case of the tensor mesons, no experimental distinction between elastic and proton - dissociative production was made in the analysis presented here. The same is true for $(\omega\pi^0)$ production. In the case of ω production a condition designed to suppress inelastic reactions was imposed, namely cuts on detectors in the forward region were applied to reject events where the proton breaks up. This cut rejects events where the mass of the forward baryonic system exceeds 1.6 GeV/c^2. The remaining background of inelastic events amounts to about 10 %.

For all but the π^0 analysis, the trigger contained, in addition to the general photoproduction tagging condition, requirements on the energy registered in the electromagnetic SpaCal. Thus, at least one SpaCal energy cluster (i.e. an isolated energy deposit, separated from neighbouring energy depositions by the clustering algorithm) had to exceed 2 GeV and at the same time have a radial distance to the beam axis of more than 16 cm. Photon candidates were reconstructed from SpaCal clusters only.

The ability to reconstruct neutral pions in the SpaCal was shown in a study on inclusive π^0 photoproduction [17]. In order to demonstrate the ability to reconstruct π^0s with the help of the VLQ, Fig. 2 shows the two-photon invariant mass for events with exactly one cluster in the SpaCal and one in the VLQ. Using the nominal interaction vertex, a clear π^0 signal is observed.

The exclusiveness of the reactions studied was ensured with the help of the variable Σ which is the sum of all $(E - P_z)$ of all particles in the electromagnetic calorimeters in the backward region, and takes a value equal to twice the electron beam energy if no particles escape undetected in the backward hemisphere. A cut of 49 GeV $< \Sigma <$ 60 GeV serves to reject non-exclusive or radiative events. For the 1996 data, the lower limit was 50 GeV.

The remaining selection criteria simply reflect the topology of the events under study: The number of photon candidates reconstructed had to equal the number of final state photons expected, and for final states with π^0's and η's, appropriate mass restrictions had to be obeyed.

3 Monte Carlo Models

The simulation programs used are PYTHIA [18] and DIFFVM [19]. The original DIFFVM event generator produces exclusive vector mesons by Pomeron exchange based on the Vector Meson Dominance model. This generator has been extended to include Odderon exchange according to the SVM with a single π^0, $f_2(1270)$, or $a_2^0(1320)$ in the final state with t-distributions for the signal processes as calculated in [9, 10]. The extended event generator is called OPIUM[1] [20].

PYTHIA is a universal tool for describing γp interactions. It is used to simulate the non-resonant $\omega\pi^0$ production (there is most likely an additional contribution from resonant $\omega\pi^0$ production via production of the $b_1(1235)$ meson which decays dominantly into these particles [5]) and the background contributing to exclusive meson production. The purely diffractive events (either Pomeron- or Odderon- induced) are modelled with the help of DIFFVM and OPIUM. The contribution from resonant $b_1(1235) \rightarrow \omega\pi^0$ was generated with the help of OPIUM where the cross section was adjusted to fit the signal observed in this analysis. The generator PYTHIA does not provide resonant b_1 production and decay. Due to the large cross section of this channel the b_1 represents a substantial background for the investigation of lower photon multiplicities if one or more photons escape detection. The final state $\omega\pi^0$ represents, through its feed-down into the four photon sample, a background source for the investigation of $f_2(1270)$ and $a_2^0(1320)$ production.

Following advice by the author of PYTHIA [18], a modified version of this program is used for the background description. Here, certain processes are excluded in which isospin conservation is not explicitly taken care of.

Contributions from Regge exchange (ω-trajectory) or $\gamma\gamma$ fusion ("Primakoff effect"), leading to elastic single pseudoscalar and tensor meson production, are negligible. A remaining background is low multiplicity events which can be modelled with the PYTHIA generator.

4 Results

In this section we discuss our results in the order dictated by the number of final state photons. The number of photons defines the C - parity of the meson produced, and thus the C - parity of the assumed exchange trajectory: an even number of photons is correlated with Odderon, an odd number with Pomeron exchange.

[1] An acronym for "Odderon and Pomeron Induced Unified Meson maker"

We first present our findings on searches for Odderon contributions to the measurement of the reaction $\gamma p \to \pi^0 N^*$. Next, we present cross section measurements for $\gamma p \to \omega p$, followed by the search for $f_2(1270)$ and $a_2^0(1320)$ production by photon - Odderon fusion. Finally, we present the cross section measurement for the reaction $\gamma p \to \omega\pi^0 X$.

Since the reaction $\gamma p \to \pi^0 N^*$ has been discussed in [16], we will repeat here only the salient features of the analysis:

Figure 3 shows the final two-photon mass distribution, with all selection criteria applied. The two dotted vertical lines indicate the two photon mass range within which π^0 candidates were accepted. The expectation from PYTHIA is four events. The Odderon-photon fusion [9], as modelled in OPIUM, predicts 110 events; 13 events are observed in the data.

Fig. 4 shows the differential cross section $d\sigma/d|t|$ for the reaction $\gamma p \to (\gamma\gamma)N^*$, where the invariant mass of the two photons lies in the pion mass region defined in Fig. 3. The squared four-momentum transfer at the nucleon vertex is approximated as $|t| = p_\perp^2(\pi^0)$. In addition, the background expectation and the SVM signal prediction are shown. Integrating the differential cross section in the accessible $|t|$ - range, i.e. for $0.02 < |t| < 0.3$ GeV^2, and applying the prescriptions of [21] and [22], one arrives at an upper limit of

$$\sigma_{\mathrm{acc}}(\gamma p \xrightarrow{\mathbb{O}} \pi^0 N^*) < 39\,\mathrm{nb} \qquad (95\ \%\ \mathrm{CL}) \qquad (1)$$

This has again to be compared with the predicted value of 200 nb at HERA energies, which is clearly incompatible with observation.

The reaction $\gamma p \to \omega p$ was investigated in the exclusive three photon sample, i.e. the ω meson was reconstructed from its decay to $\pi^0\gamma$. Fig. 5 shows the two-photon invariant mass distribution, with a clear π^0 signal. Also shown are the expectations from the signal (DIFFVM) and background Monte Carlo simulations (PYTHIA and feed-down from b_1 and non-resonant $\omega\pi^0$ production). ¿From this distribution a π^0 mass window is derived which is defined by $|m_{\gamma\gamma} - m_{\pi^0,\mathrm{PDG}}| < 40$ MeV/c^2.

The three photon invariant mass distribution, where one photon pair is required to have its invariant mass in the π^0 mass window, is displayed in Fig. 6 and shows the ω signal. In addition, the signal and background Monte Carlo expectations are shown.

The cross section was determined by fitting the line shape and subtracting the non - ω background statistically. The background was determined with the PYTHIA and OPIUM Monte Carlo programs. The latter is used to desribe the feed-down from b_1 decays into five photons where two photons have not been detected. In addition, a remaining background of 10 % inelastic ω production was removed. The cross section then amounts to

$$\sigma(\gamma p \to \omega p) = (1.25 \pm 0.17\ (\mathrm{stat}) \pm 0.22\ (\mathrm{syst}))\ \mu\mathrm{b}.$$

The four - momentum transfer squared ($|t|$-) distribution for the reaction $\gamma p \to \omega p$ at the proton vertex (with the approximation $|t| = p_\perp^2(\omega)$) is shown in Fig. 7. Events subjected to the fit were chosen to be ω - candidates , i.e. they had to fulfil the requirement $0.65 < m_{\pi^0\gamma} < 1.00$ GeV/c^2. A fit of an exponential of the form $dN/d|t| = A\ \exp(-b|t|)$ to the data in the range $|t| < 0.4$ GeV^2, gives a slope of

$$b = (10.5 \pm 1.2\ (\mathrm{stat}) \pm 0.5\ (\mathrm{syst}))\ \mathrm{GeV}^{-2}$$

which is in the range typical for elastic vector meson photoproduction at this energy. Fig. 8 shows the slope values measured for elastic diffractive ω photoproduction reactions, and Fig. 9 shows the partial cross sections for diffractive photoproduction cross sections, as a function of the photon - proton centre-of-mass energy W. One observes that the values presented in this paper fit excellently in the general pattern.

The exclusive four photon sample was searched for evidence of Odderon exchange leading to $f_2(1270)$ and $a_2^0(1320)$ production. Fig. 10 shows the invariant mass of all $\gamma\gamma$ pairs, together with the sum of the signal Monte Carlo predictions for $f_2(1270)$ and $a_2^0(1320)$ and the background Monte Carlo expectation (PYTHIA and feed-down from b_1 and non-resonant $\omega\pi^0$ production). A π^0 signal is visible but weaker than expected from the SVM. Fig. 11 shows an extended two photon invariant mass distribution, this time the $\gamma\gamma$ system "recoiling" against the π^0 which is defined by an invariant mass cut as above. According to the Odderon exchange models, in this plot, a second π^0 signal is expected in the case of $f_2(1270)$, and an η signal in the case of $a_2^0(1320)$ production. No η and less π^0's are seen than expected in OPIUM. The expected signals are also shown in the figure. The data distribution is compatible with the bare background expectation. The same conclusion can be drawn from the π^0 - η invariant mass distribution shown in Fig. 12 where the π^0 mass range definition is as above, and the η region is defined by $|m_{\gamma\gamma} - m_{\eta,\mathrm{PDG}}| < 100$ MeV/c^2. The signal prediction from the SVM is added. Again, the data distribution is compatible with the background expectation. Finally, the two π^0 invariant mass distribution is presented in Fig. 13. The data is shown together with the background Monte Carlo expectation and the $f_2(1270)$ SVM prediction.

Converting the findings of the exclusive four photon analysis into numbers, one arrives, applying again the prescriptions of [21] and [22], at the following limit for $a_2^0(1320)$ production:

$$\sigma(\gamma p \xrightarrow{\mathbb{O}} a_2 X) < 96\,\mathrm{nb} \qquad (95\ \%\ \mathrm{CL})$$

to be compared with the SVM prediction for $\sigma(\gamma p \xrightarrow{\mathbb{O}} a_2 N^*) = 190\,\mathrm{nb}$. The corresponding numbers for $f_2(1270)$ production

$$\sigma(\gamma p \xrightarrow{\mathbb{O}} f_2 X) < 16\,\mathrm{nb} \qquad (95\ \%\ \mathrm{CL})$$

are to be compared with the model prediction $\sigma(\gamma p \xrightarrow{\mathbb{O}} f_2 N^*) = 21\,\mathrm{nb}$.

Finally we discuss the five photon sample. Fig. 14 shows the invariant mass of all ten $\gamma\gamma$ combinations with a clear π^0 signal. The data distribution is compared with the sum of the background expectation (PYTHIA, non-resonant $\omega\pi^0$ production, and contribution from $b_1 \to \omega\pi^0$ where the ω decays into $\pi^+\pi^-\pi^0$) and the prediction of a signal Monte Carlo for $b_1(1235)$ production. The b_1 decays dominantly to $\omega\pi^0$ and hence can produce purely photonic final states. Fig. 15 shows the three photon invariant mass "recoiling" against the π^0. A clear ω peak is observed. For further analysis, the ω mass range is defined by $|m_{3\gamma} - 0.76$ GeV/c$^2| < 0.15$ GeV/c^2. The ω central mass results from the fit which also served to derive the $\omega\pi^0$ cross section by determining the number of ω's in the sample. The shape of the $\omega\pi^0$ invariant mass distribution displayed in Fig. 16 shows very good agreement with the model prediction. The absolute normalization of the resonant b_1 contribution to the $\omega\pi^0$ final state has been taken from the OPIUM generator which was adjusted to fit the observed data. The non-resonant contribution is taken from the PYTHIA prediction. The conclusion is that there is substantial $\omega\pi^0$ diffractive photoproduction which might well proceed via dominant resonant $b_1(1235)$ production. The corresponding cross section is

$$\sigma(\gamma p \to \omega\pi^0 X) = (980 \pm 200\ (\mathrm{stat}) \pm 200\ (\mathrm{syst}))\ \mathrm{nb}.$$

This has to be compared with the sum of the non-resonant prediction by PYTHIA

$$\sigma_{\mathrm{PYTHIA}}(\gamma p \to \omega\pi^0 X) = 190\ \mathrm{nb}$$

and a cross section value measured for b_1 photoproduction at lower energies (8 GeV, [4]) which, after extrapolation to HERA energies reads

$$\sigma_{extrap}(\gamma p \to b_1 p) = (660 \pm 250)\ \mathrm{nb}.$$

The extrapolation followed [7, 8] in complete analogy to the ordinary vector mesons with the $\gamma I\!\!P V$ coupling adapted to match the low energy data.

5 Conclusion

Our findings provide a rather clear picture. We have observed Pomeron induced reactions in complete agreement with previous measurements, expectations, and extrapolations from lower energy experiments, but: we see no trace of Odderon induced reactions as predicted by the Stochastic Vacuum Model (SVM).

Possible explanations include:

1. The energy dependence of the cross section is different from that assumed. This would imply that the Odderon intercept $\alpha_{\mathbb{O}}(0)$ is considerably smaller than one. A value of $\alpha_{\mathbb{O}}(0) < 0.65$ would be compatible with the π^0 cross section limit, but this would mean that the object exchanged is not a "genuine" Odderon for which $\alpha_{\mathbb{O}}(0) \approx 1$.

2. The absence of elastic π^0 production could be understood in that the coupling at the $\gamma\mathbb{O}\pi$-vertex is small due to the Goldstone Boson nature of the π^0 [23]. This explanation does, however, not hold in the case of the $f_2(1270)$ and the $a_2(1320)$.

The level of understanding of this sector of nonperturbative QCD is still unsatisfactory, and new theoretical ideas are needed.

Acknowledgements

We are grateful to the HERA machine group whose outstanding efforts have made and continue to make this experiment possible. We thank the engineers and technicians for their work constructing and maintaining the H1 detector, our funding agencies for financial support, the DESY technical staff for continuous assistance, and the DESY Directorate for the hospitality which they extend to the non-DESY members of the collaboration. For many stimulating and helpful discussions, the authors wish to thank E. R. Berger, H. G. Dosch, O. Nachtmann, and T. Sjöstrand.

References

[1] I. Ya. Pomeranchuk, Zh. Eksp. Teor. Fiz. **34** (1958) 725, and Sov. Phys. JETP **7** (1958) 499.

[2] L. Lukaszuk and B. Nicolescu, Lett. Nuov. Cim. **8** (1973) 405.

[3] D. Joynson, E. Leader, B. Nicolescu, C. Lopez, Nuov. Cim. **30A** (1975) 345.

[4] The Omega Photon Collaboration, M. Atkinson et al., Nucl. Phys. **B243** (1984) 1; ZEUS Collaboration, M. Derrick et al., Z. Phys. **C73** (1996) 73

[5] The Particle Data Group, D. E. Groom et al., Eur. Phys. J. **15** (2000) 1

[6] A. Donnachie and P. V. Landshoff, Phys. Lett. **B296** (1992) 227.

[7] J. Cudell et al., Phys. Rev. **D61** (2000) 34019

[8] G. A. Schuler and T. Sjöstrand, Nucl. Phys. **B407** (1993) 539.

[9] E. R. Berger, A. Donnachie, H. G. Dosch, W. Kilian, O. Nachtmann, M. Rüter, Eur. Phys. J. **C9** (1999) 491; E. R. Berger et al., Eur. Phys. J. **C14** (2000) 673.

[10] H. G. Dosch, private communication

[11] H. G. Dosch and Yu. A. Simonov, Phys. Lett. **B205** (1988) 339.

[12] O. Nachtmann, Ann. Phys. **209** (1991) 436.

[13] H1 Coll., I. Abt et al., Nucl. Instrum. Methods **A386** (1997) 310 and 348.

[14] H1 SpaCal Group, T. Nicholls et al., Nucl. Instrum. Methods **A374** (1996) 149; H1 SpaCal Group, R.D. Appuhn et al., Nucl. Instrum. Methods **A382** (1996) 395; H1 SpaCal Group, R.D. Appuhn et al., Nucl. Instrum. Methods **A386** (1997) 397.

[15] M. Keller et al., Nucl. Instr. Methods **A409** (1998) 604.

[16] H1 Collaboration, "Search for Odderon Induced Contributions to Exclusive π^0 Photoproduction at HERA", to appear in the Proceedings of the 9th International Workshop on Deep Inelastic Scattering DIS2001, Bologna, 27 April - 1 May, 2001.

[17] C. Adloff et al., H1 - Collaboration, Eur. Phys. J. **C18** (2000) 29

[18] T. Sjöstrand, Comp. Phys. Comm. **82** (1994) 74; private communication (2001).

[19] B. List and A. Mastroberardino, "DIFFVM - A Monte Carlo Generator for Diffractive Processes in ep Scattering", available as: `http://www.desy.de/~heramc/mclist.html.`

[20] W. Kornelis, private communication, Heidelberg (2000).

[21] R. D. Cousins and G. J. Feldman, Phys. Rev. **D57** (1998) 3873.

[22] R. D. Cousins and V. L. Highland, Nucl. Instr. Meth. **A320** (1992) 331.

[23] O. Nachtmann, private communication, Heidelberg (2001).

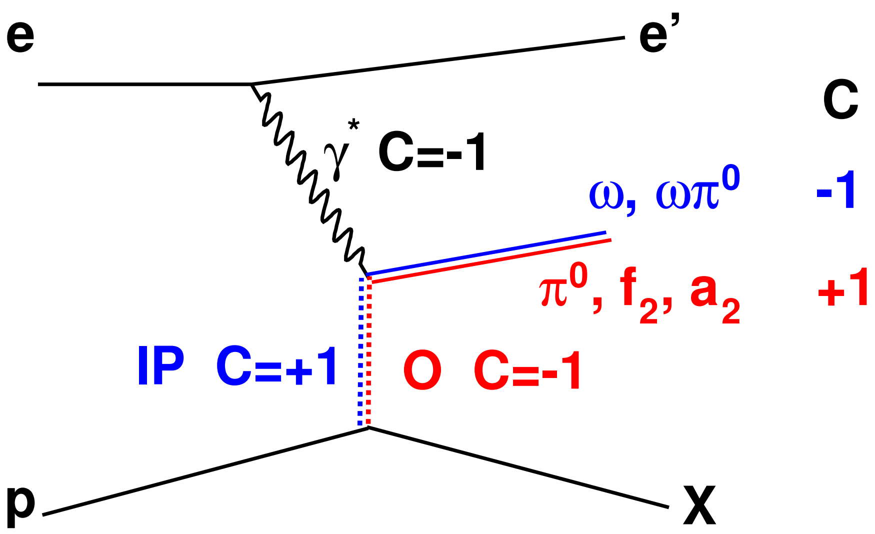

Figure 1: Generic diagram illustrating photon - Pomeron and photon - Odderon induced exclusive processes.

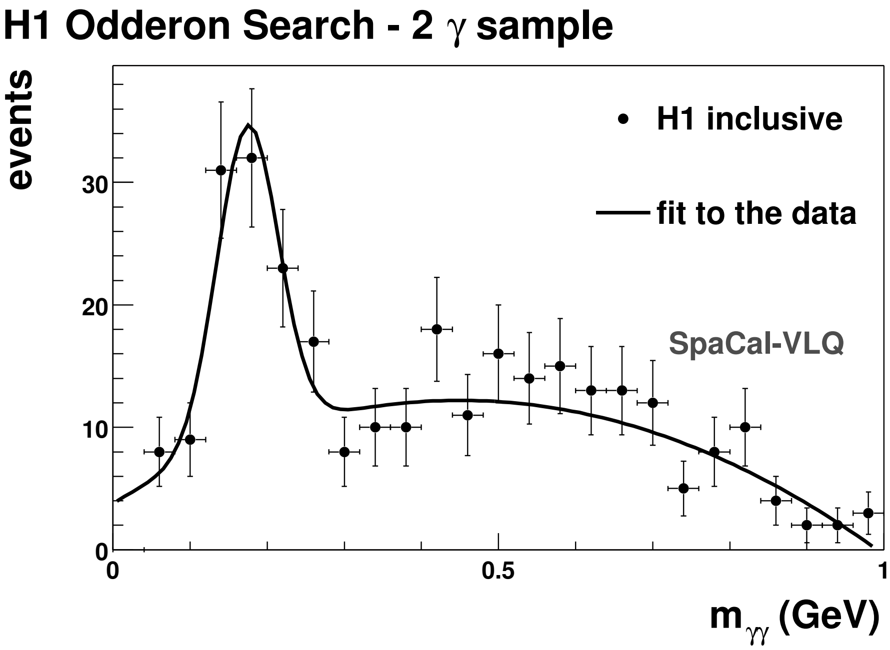

Figure 2: Two photon sample: Invariant mass spectrum of the two-photon candidates for events where one photon is detected in the VLQ and one in the SpaCal. In addition, a neutron and the scattered electron are detected. The full line shows the result of a fit of a Gaussian plus a fourth order polynomial.

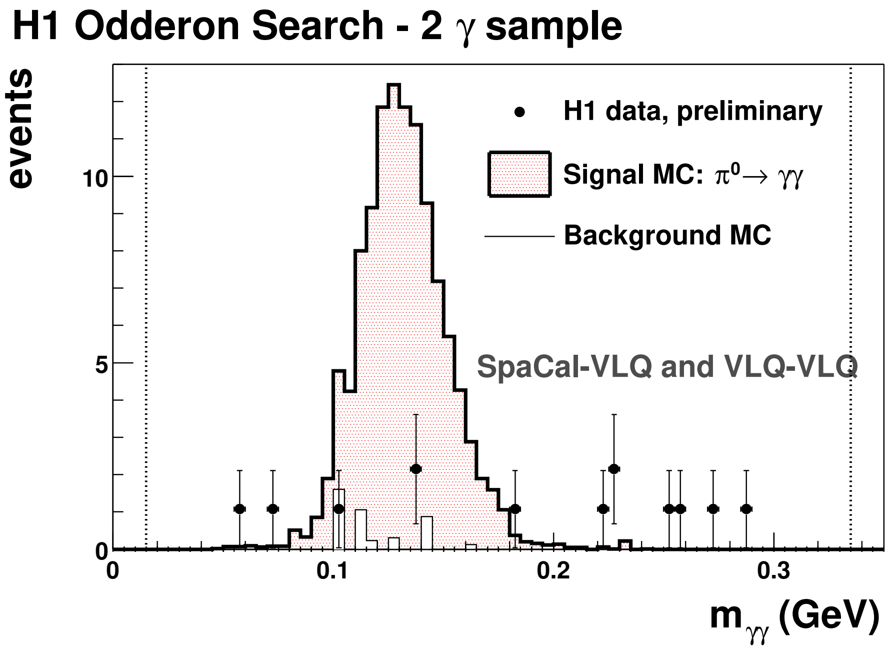

Figure 3: Two photon sample: Distribution of two photon invariant mass, with either both photons detected in the VLQ, or one photon detected in the VLQ and the second one in the SpaCal, after all selection cuts. Also shown are the model expectation (hatched area) and the prediction from the background MC (white histogram). The two vertical lines indicate the mass region for π^0 candidates.

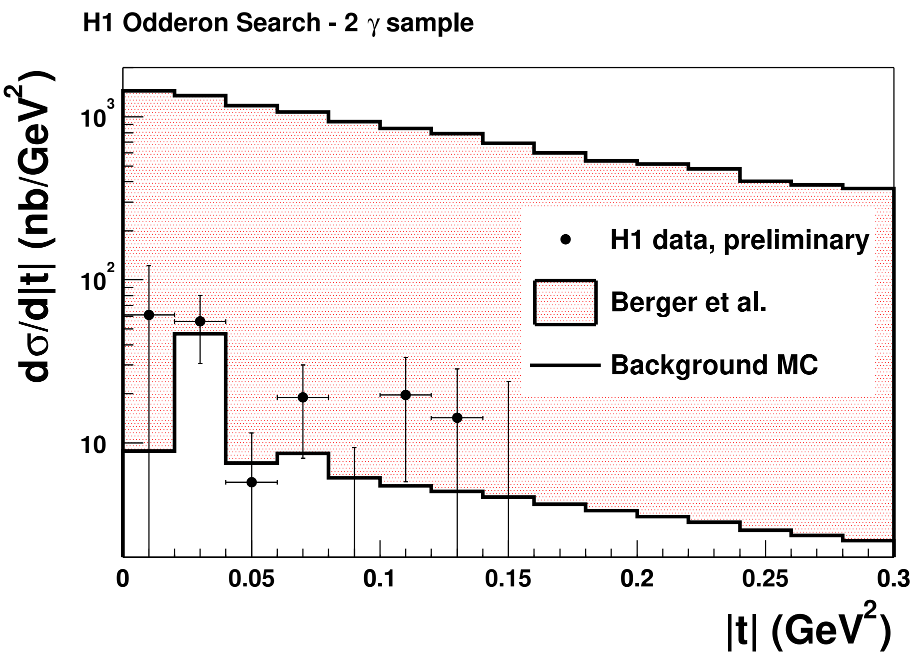

Figure 4: Differential cross section for the reaction $\gamma p \to (\gamma\gamma)N^*$, with the two photon invariant mass inside the π^0 candidate range (see text). Also shown are the background Monte Carlo expectation and the SVM signal prediction.

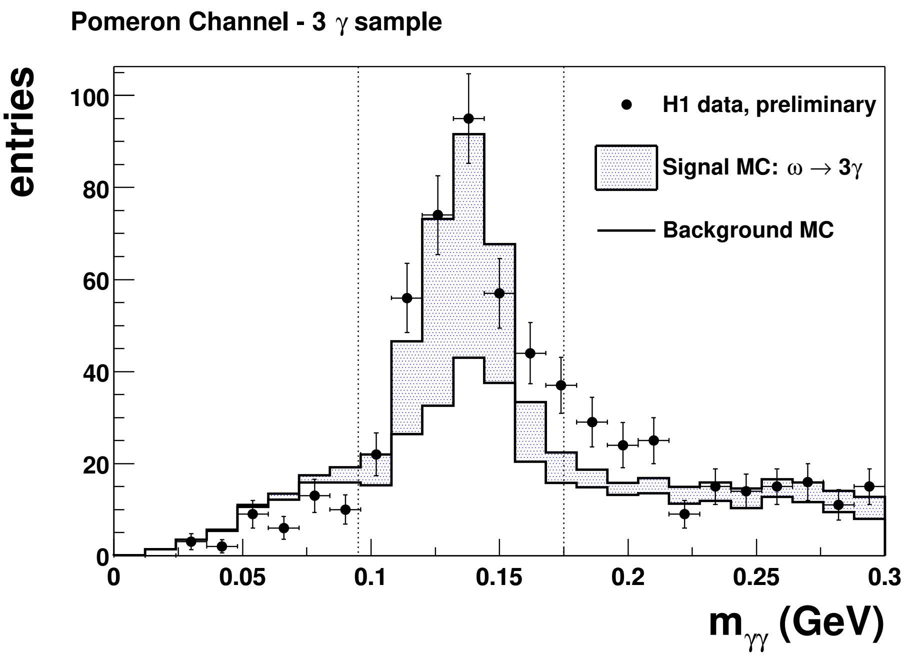

Figure 5: Three photon sample: Two photon invariant mass distribution, for data, background Monte Carlo (see text), and model expectation.

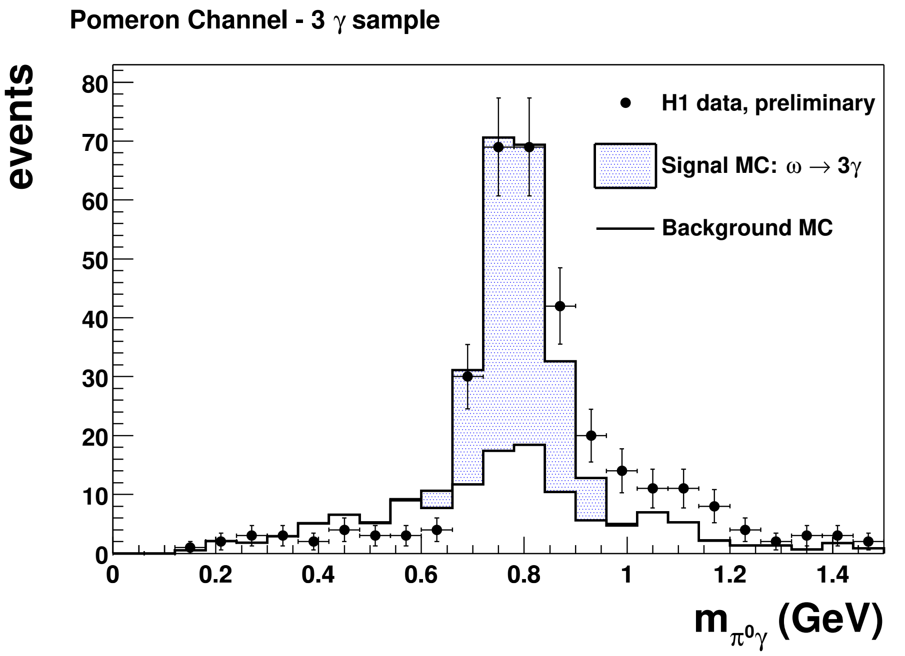

Figure 6: Three photon sample: Three photon invariant mass distribution, with one $\gamma\gamma$ invariant mass in the π^0 mass window, for data, background Monte Carlo (see text), and model expectation.

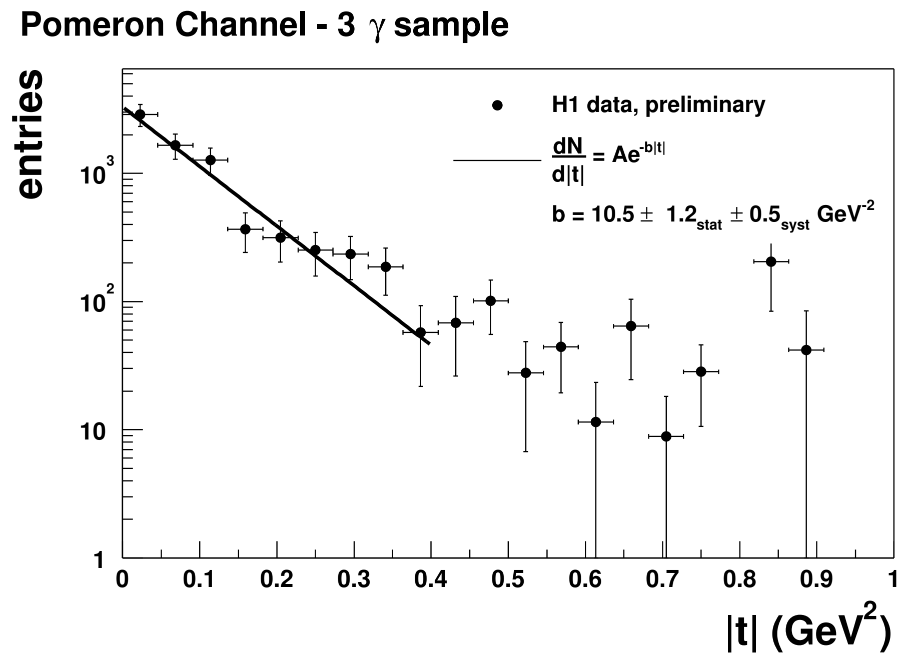

Figure 7: Three photon sample: Distribution of four - momentum transfer squared ($|t|$) at the proton vertex. The full line shows the result of a fit of an exponential $|t|$ - distribution to the data.

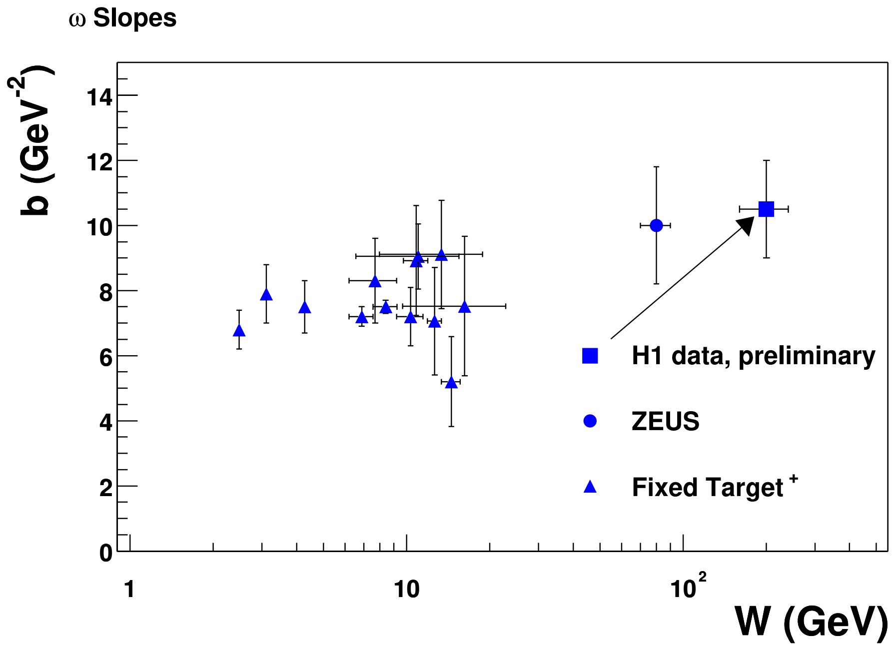

Figure 8: A compilation of slopes of $|t|$ - distributions for elastic ω photoproduction as a function of the photon - proton centre-of-mass energy, from fixed target to HERA experiments.

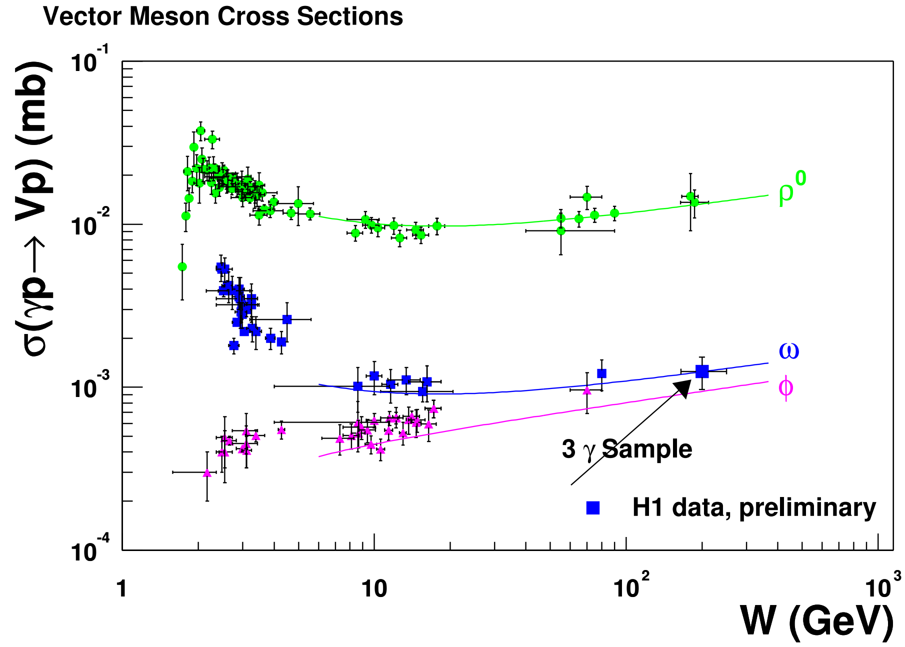

Figure 9: A synopsis of elastic vector meson photoproduction cross sections as a function of the photon - proton centre-of-mass energy, from fixed target to HERA experiments.

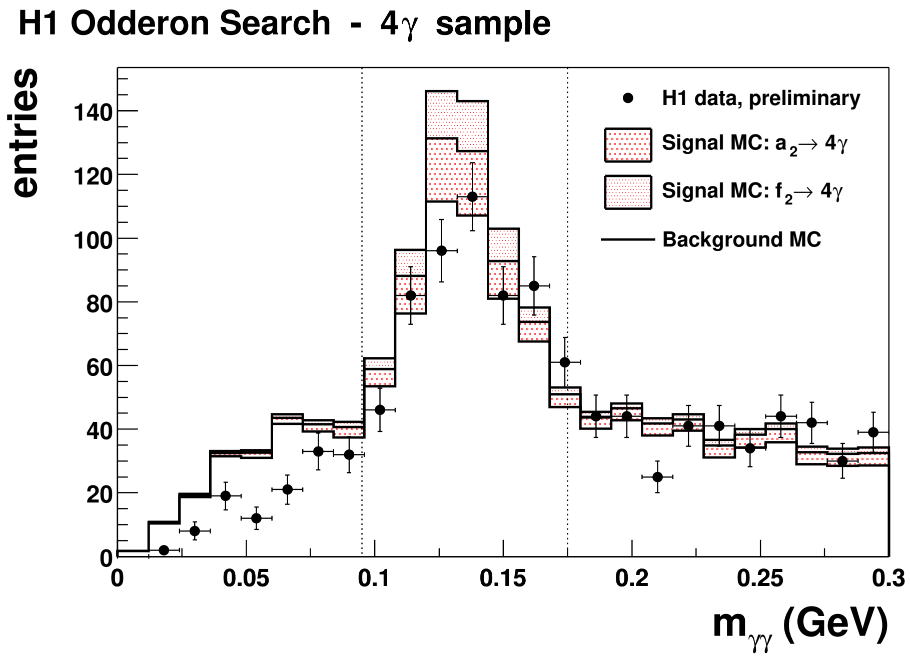

Figure 10: Four photon sample: Two photon invariant mass distribution, for data, background Monte Carlo (see text), and model expectations.

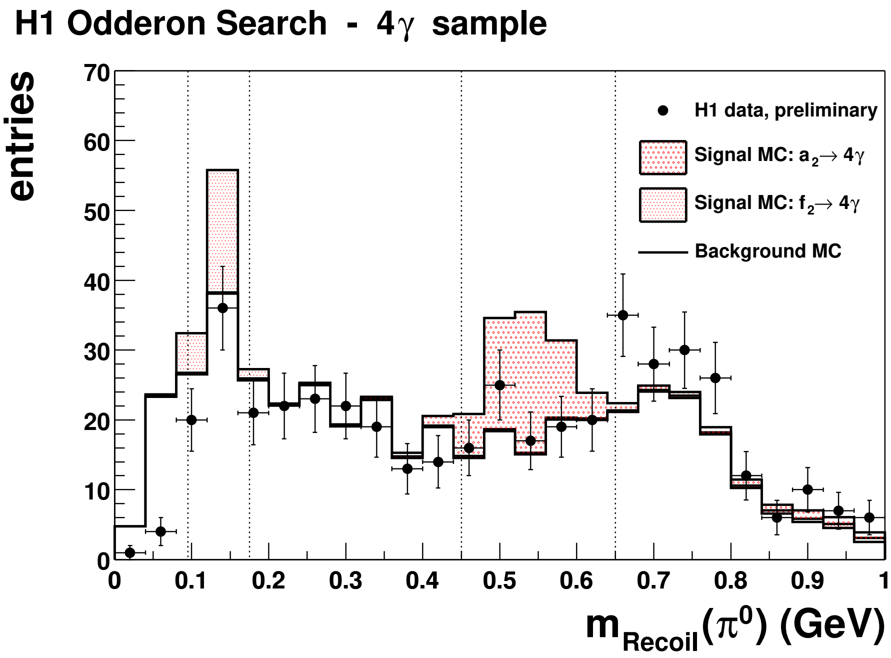

Figure 11: Four photon sample: Two photon invariant mass "recoiling" against π^0, for data, background Monte Carlo (see text), and model expectations.

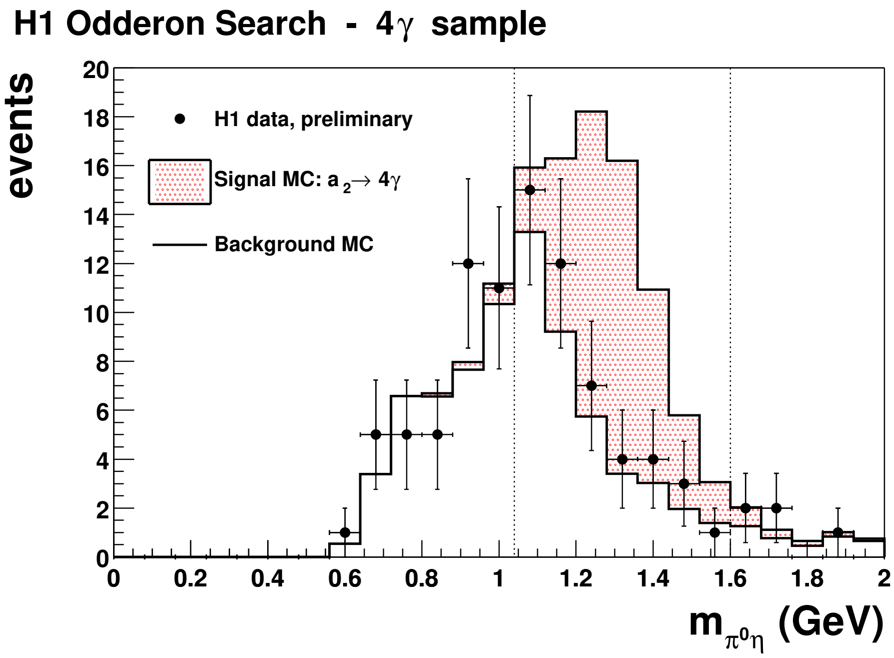

Figure 12: Four photon sample: π^0 - η invariant mass, for data, background Monte Carlo (see text), and model expectation. For π^0 and η mass definitions, see text.

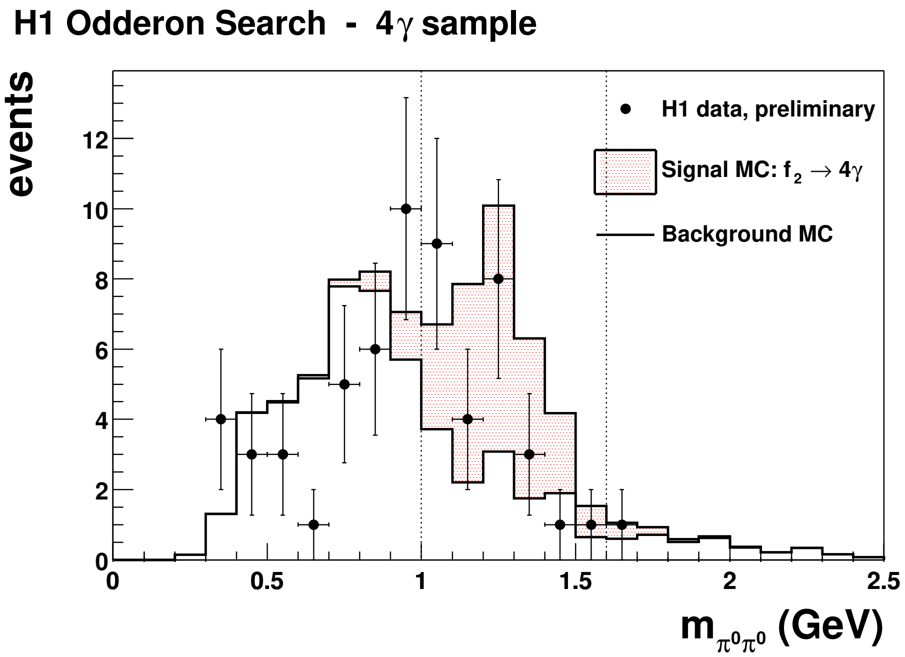

Figure 13: Four photon sample: Two π^0 invariant mass distribution, for data, background Monte Carlo (see text), and model expectations. For π^0 mass definition, see text.

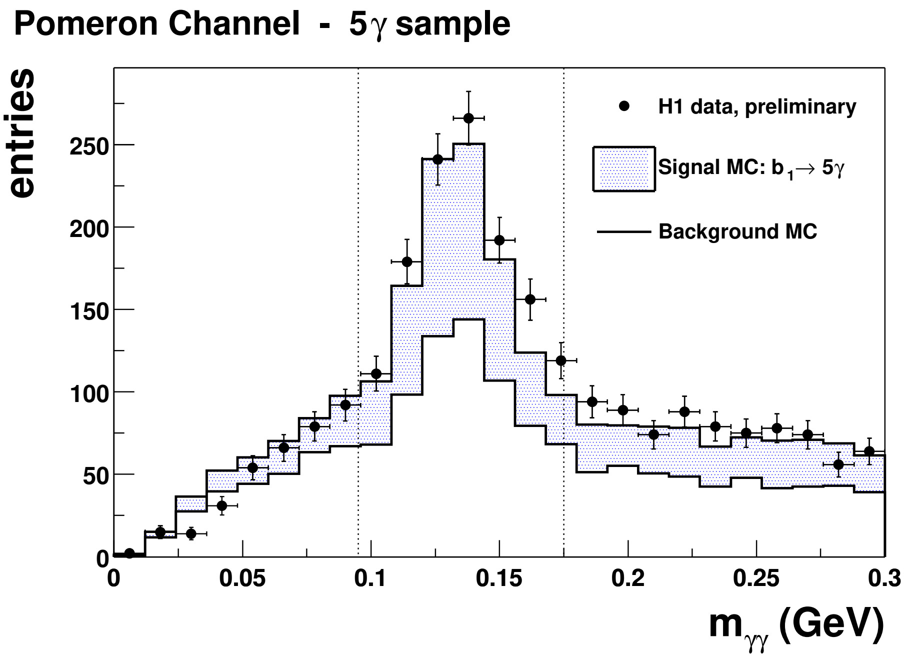

Figure 14: Five photon sample: Two photon invariant mass distribution for data, background Monte Carlo (see text), and model expectations (ten entries per event).

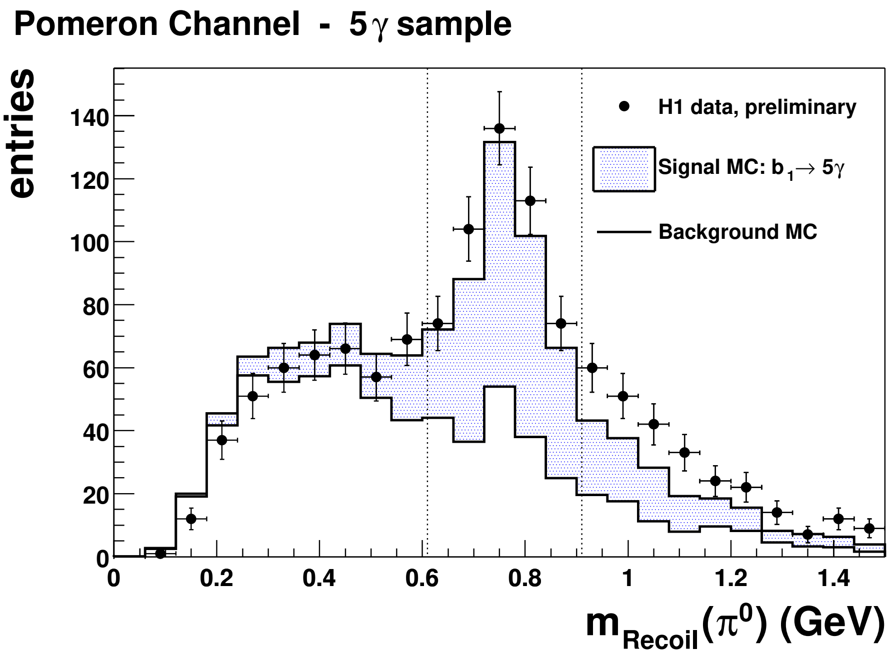

Figure 15: Five photon sample: Three photon invariant mass "recoiling" against π^0, for data, background Monte Carlo (see text), and model expectations. For ω mass definition, see text.

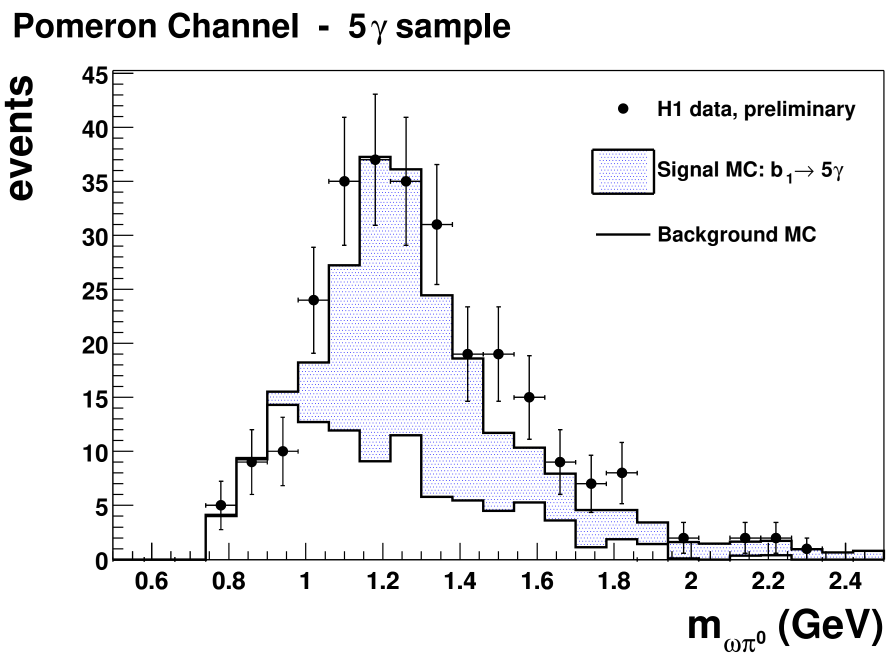

Figure 16: Five photon sample: ω - π^0 invariant mass, for data, background MC (see text), and model expectation. For ω and π^0 mass definitions, see text.